Thermochimica Acta, 232 (1994) 65–76
Elsevier Science B.V., Amsterdam
SSDI 0040-6031(93)01377-F

A study of the thermal decomposition of ammine zinc hydroxide nitrates

P. Bénard, J.P. Auffrédic * and D. Louër

Laboratoire de Cristallochimie (URA CNRS 1495), Université de Rennes I, Avenue du Général Leclerc, 35042 Rennes Cédex (France)

(Received 16 April 1993; accepted 24 May 1993)

Abstract

A new diammine zinc hydroxide nitrate, $Zn_5(OH)_8(NO_3)_2 \cdot 2NH_3$ and a new aquo-ammine zinc hydroxide nitrate, $Zn_5(OH)_8(NO_3)_2 \cdot 1.3NH_3 \cdot 0.7H_2O$, isostructural with $Zn_5(OH)_8(NO_3)_2 \cdot 2H_2O$, have been synthesized. It is demonstrated that the thermal decomposition process of these three compounds into ZnO, investigated by means of thermogravimetry, thermodiffractometry and mass spectrometry, depends upon the substitution rate of H_2O by NH_3 molecules. The diammine compound decomposes in two stages and the two others in three stages. A new ammine zinc hydroxide nitrate with the proposed chemical formula $Zn(OH)(NO_3) \cdot NH_3$ is formed in the first stage of the decomposition of the ammines. It has been characterized by its X-ray powder diffraction pattern. The formation of $Zn_3(OH)_4(NO_3)_2$ during the decompositions requires that the compounds are hydrated. However, the anhydrous solid $Zn_5(OH)_8(NO_3)_2$ is obtained only from the dihydrated hydroxysalt.

INTRODUCTION

A number of zinc hydroxide nitrates have a layer structure derived from the brucite type structure [1]. Some of them have been used as precursors of zinc oxide whose specific microstructural properties, e.g. shape, size and distribution of crystallite sizes, have been determined from precise X-ray diffraction line profile analysis [2, 3]. The compound $Zn_5(OH)_8(NO_3)_2 \cdot 2H_2O$ belongs to the type IIb of the structural classification of divalent metal hydroxide nitrates [1]. Its structure [4] consists of infinite brucite type layers, parallel to the (100) plane of the monoclinic cell, where one quarter of the zinc atoms in octahedral interstices are removed from the layer. On either side of the empty octahedra, are located Zn atoms tetrahedrally coordinated by the ions OH^- and water molecules. The nitrate groups situated between the sheets are not involved in the coordination of the zinc atoms. They can be easily substituted by the anions

* Corresponding author.

Cl^- through a topotactic reaction without important structural modifications [5]. It was of interest to investigate the exchange of water molecules by another neutral group such as ammonia and to study the subsequent effects on the structural properties and the thermal decomposition process of the resulting compounds.

The present paper deals with the synthesis of two new ammine zinc hydroxide nitrates of formula $Zn_5(OH)_8(NO_3)_2 \cdot (2-x)NH_3 \cdot xH_2O$ ($x = 0$ and 0.7), whose crystal structures, reported elsewhere [6], are derived from the type IIb by substituting NH_3 for H_2O molecules. Their thermal decomposition process, investigated by means of thermodiffractometry, thermogravimetry and mass spectrometry, is reported and compared with that of $Zn_5(OH)_8(NO_3)_2 \cdot 2H_2O$.

EXPERIMENTAL

Sample preparation

The materials investigated in this study were prepared as follows.

(i) $Zn_5(OH)_8(NO_3)_2 \cdot 2H_2O$ has been obtained from a slow hydrolysis of a 2 M solution of zinc nitrate [4].

(ii) Crystals of aquo-ammine zinc hydroxide nitrate, $Zn_5(OH)_8(NO_3)_2 \cdot 1.3NH_3 \cdot 0.7H_2O$, were produced by using an interdiffusion method [7], based on the diffusion of ammonia in an aqueous zinc nitrate solution. By means of a pipette, 15 cm^3 of a 2 M solution of zinc nitrate were introduced at the bottom of a glass tube (5 cm diameter) containing 30 cm^3 of water. This tube was connected to another one containing a 6 M solution of ammonia. The synthesis was performed at 14°C. After about ten days, needle shape crystals grew from the wall of the first tube. For these crystals the Zn content and the total amount of the basic groups, OH^- and NH_3, were determined by EDTA and acidimetric titrations, respectively. The total mass loss to ZnO ($\Delta m/m_0$) was obtained from TG measurement. From the results (Table 1), the chemical formula of the crystals was determined as $Zn_5(OH)_8(NO_3)_2 \cdot 1.3NH_3 \cdot 0.7H_2O$.

(iii) The diammine phase was obtained by slowly evaporating, at 30°C, a 1.5 M solution of zinc nitrate in 12 M ammonia. After about 20 h, piles of

TABLE 1

Chemical analysis results for ammine zinc hydroxide nitrates

Sample	Zn^{2+} in %	$n(OH^- + NH_3)$	$\Delta m/m_0$ in %
$Zn_5(OH)_8(NO_3)_2 \cdot 1.3NH_3 \cdot 0.7H_2O$	53.0	9.3	34.0
$Zn_5(OH)_8(NO_3)_2 \cdot 2NH_3$	53.0 (52.68) [a]	9.96 (10) [a]	34.4 (34.4) [a]

[a] Values in parentheses are theoretical calculated values.

small crystals were formed inside the solution at the bottom and on the wall of the glass container. They were repeatedly washed with water and alcohol and then dried at 40°C. The results of their chemical analysis (Table 1) agree well with the chemical formula $Zn_5(OH)_8(NO_3)_2 \cdot 2NH_3$.

Thermogravimetry

TG curves were recorded with a "Thermoflex" instrument (Rigaku Denki Co.). In order to avoid mass effects and to reproduce as much as possible the experimental conditions used in thermodiffractometry, about 20 mg of powdered sample were spread evently in a large platinum crucible 15 mm in length, 10 mm in width and 1 mm in height. The sample was heated at a rate of $10°C\,h^{-1}$ in nitrogen flowing at a rate of $40\,ml\,min^{-1}$.

X-ray powder diffraction

Thermodiffractometry was carried out by means of an X-ray diffractometer equipped with a high-temperature furnace attachment combined with an INEL (CPS 120) curved position sensitive detector (PSD) which allows for a simultaneous data recording of a diffraction pattern over a range of 120°. Monochromatic Cu $K\alpha_1$ radiation was selected by means of an incident beam monochromator. The details concerning this arrangement have been described elsewhere [8]. To ensure satisfactory counting statistics, an interval time of 1150 s between two successive powder diffraction patterns was selected, including a counting time of 1000 s.

For precise powder diffraction data collection, a D500 Siemens powder X-ray diffraction system was used. Pure Cu $K\alpha_1$ radiation was produced with an incident-beam curved-crystal germanium monochromator with asymmetric focussing. Details concerning the accuracy and the instrumental resolution have been discussed elsewhere [9].

Determination of X-ray diffraction line positions and integrated intensities was carried out by means of the fitting program FIT, available in the PC software package DIFFRAC-AT supplied by Siemens/Socabim.

Mass spectrometry

The analysis of the gas evolved from the solids in the course of their thermal decomposition was carried out by using a Varian 311 mass spectrometer. A few micro-crystals were placed in a reaction chamber near

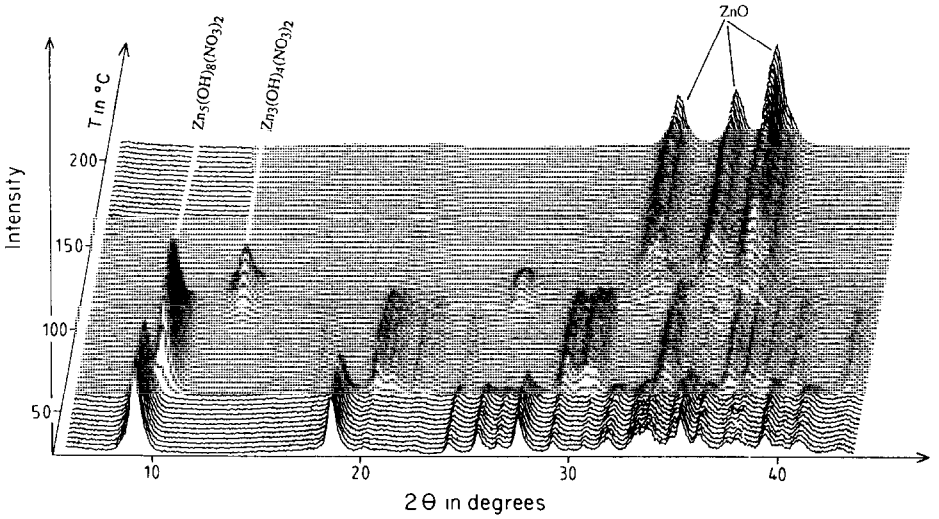

Fig. 1. X-Ray diffraction 3D plot for the decomposition of $Zn_5(OH)_8(NO_3)_2 \cdot 2H_2O$ in nitrogen gas (heating rate, 10°C h^{-1}; counting time for each pattern, 1000 s).

the ionization source under a pressure of 10^{-7} mbar and submitted to thermal decomposition at a heating rate of 200°C h^{-1}.

RESULTS

Thermal decomposition of $Zn_5(OH)_8(NO_3)_2 \cdot 2H_2O$

Figure 1 shows the 3D plot of the successive powder diffraction patterns in the temperature range 20–220°C at 3.2°C intervals. The TG curve and the integrated intensity of a selected diffraction line for each compound as a function of temperature are shown in Fig. 2. The results are in agreement with a previous study [10] in which it was stated that the decomposition proceeds through three stages with the successive formation of $Zn_5(OH)_8(NO_3)_2$, a mixture of $Zn_3(OH)_4(NO_3)_2$ and ZnO, and ZnO. However, the TG curve shows the slow release of the gaseous products, due to adsorption effects, which is only complete at 300°C, while the total structural transformation is achieved at about 170°C.

Thermal decomposition of $Zn_5(OH)_8(NO_3)_2 \cdot 2NH_3$

The results of thermodiffractometry and TG analyses are shown in Figs. 3 and 4. They demonstrate that $Zn_5(OH)_8(NO_3)_2 \cdot 2NH_3$ decomposes into ZnO through two stages. The first one takes place in the temperature range 85–115°C and is characterized by the simultaneous formation of ZnO and a new compound which has been called phase X. The second one, which occurs between 120 and 155°C, corresponds to the decomposition of phase

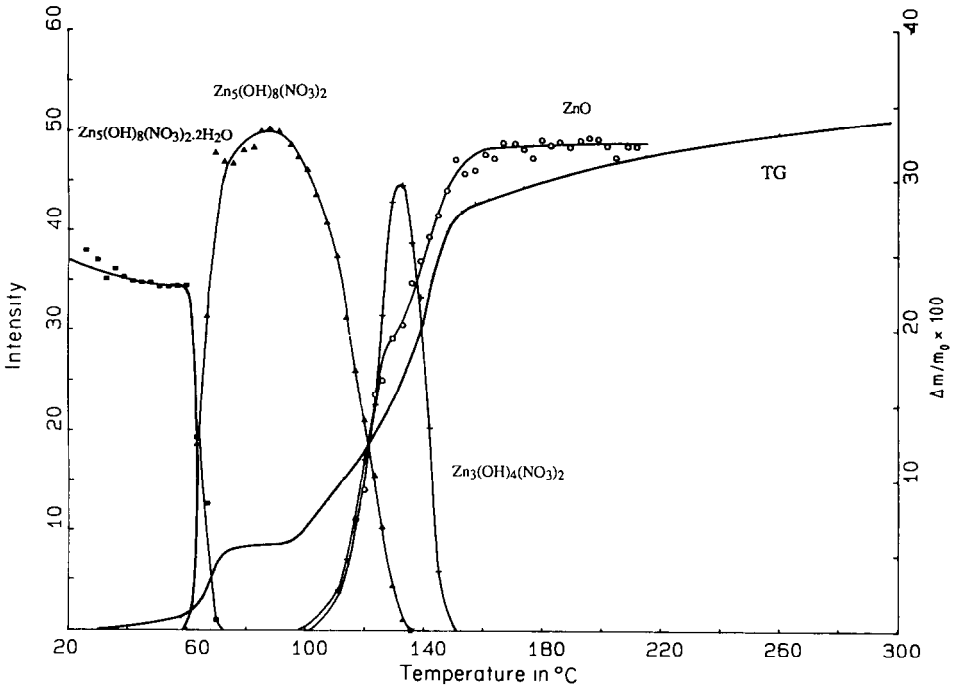

Fig. 2. Integrated intensities of selected diffraction lines vs. temperature from the thermodiffractometry of $Zn_5(OH)_8(NO_3)_2 \cdot 2H_2O$ in nitrogen gas (■, 200 of $Zn_5(OH)_8(NO_3)_2 \cdot 2H_2O$; △, 200 of $Zn_5(OH)_8(NO_3)_2$; +, 100 of $Zn_3(OH)_4(NO_3)_2$; ○, 002 of ZnO). The full line represents the TG curve.

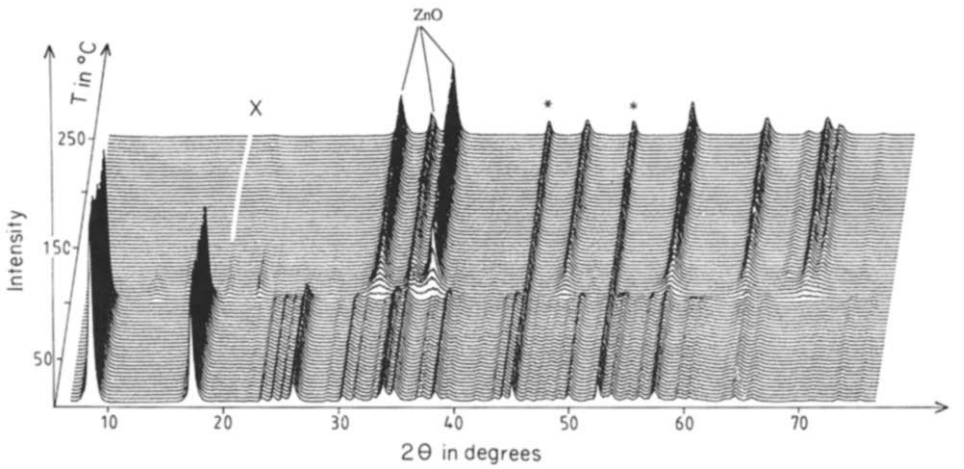

Fig. 3. X-Ray diffraction 3D plot for the decomposition of $Zn_5(OH)_8(NO_3)_2 \cdot 2NH_3$ in nitrogen gas (heating rate, 10°C h^{-1}; counting time for each pattern, 1000 s); *, spurious diffraction lines due to the sample holder being nickel.

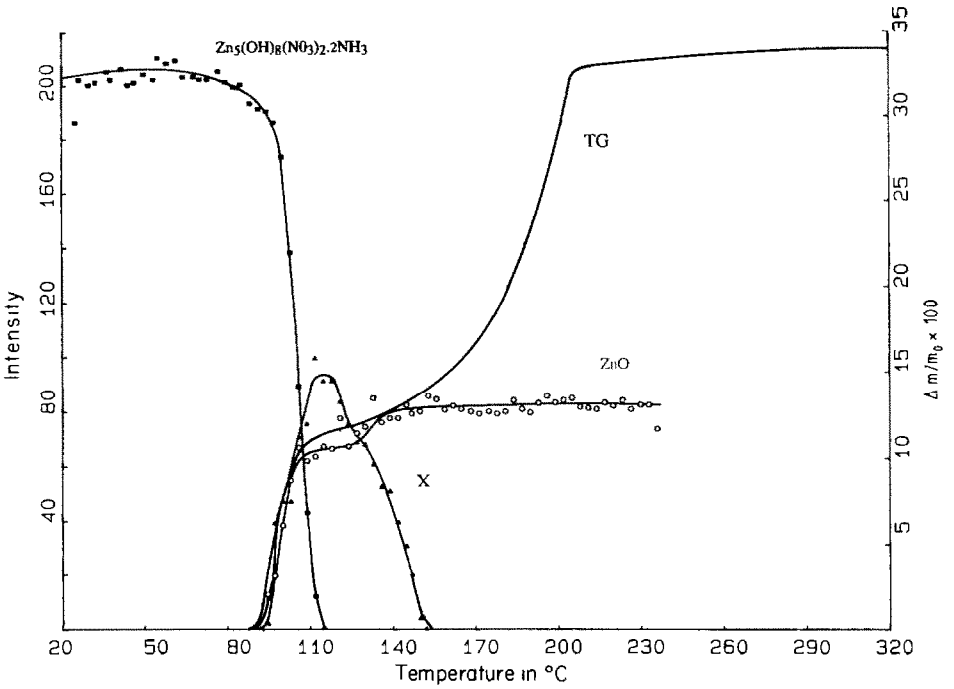

Fig. 4. Integrated intensities of selected diffraction lines vs. temperature from the thermodiffractometry of $Zn_5(OH)_8(NO_3)_2 \cdot 2NH_3$ in nitrogen gas (■, 200 of $Zn_5(OH)_8(NO_3)_2 \cdot 2NH_3$; ▲, 021 of X; ○: 100 of ZnO). The full line represents the TG curve.

X into ZnO. From the TG curve, it can be seen that the mass loss is complete at temperature greater than 260°C. This should be attributed to the adsorption of gaseous products on the finely divided ZnO formed at low temperature and to their further desorption at higher termperature. It is likely that this adsorption phenomenon takes place from the first stage since the formation of ZnO necessarily involves the destruction of some nitrate groups. Hence the TG curve cannot provide valuable information about the composition of the new compound X. However, as deduced from the variation of the intensity of the X-ray diffraction line 100 of ZnO as a function of temperature, about 80% of the total amount of ZnO is obtained at the end of the first stage. Consequently, it can be concluded that phase X produces about 20% of the total amount of ZnO in the second stage, i.e. one molecule of ZnO.

Thermal decomposition of $Zn_5(OH)_8(NO_3)_2 \cdot 1.3NH_3 \cdot 0.7H_2O$

From Figs. 5 and 6, it can be seen that the thermal decomposition of this compound into ZnO proceeds through three stages. The first occurs between 90 and 125°C and corresponds to the simultaneous formation of

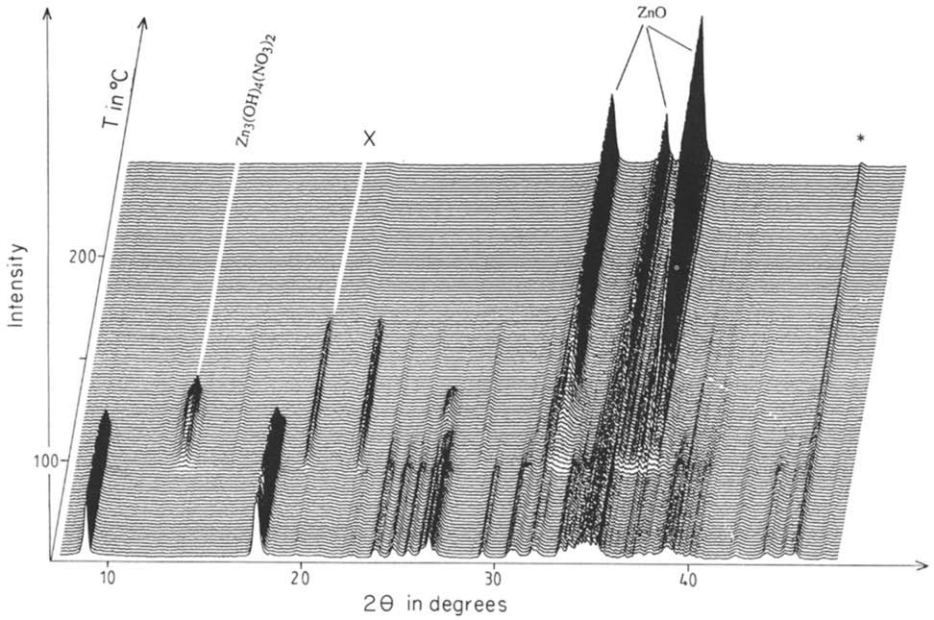

Fig. 5. X-ray diffraction 3D plot for the decomposition of $Zn_5(OH)_8(NO_3)_2 \cdot 1.3NH_3 \cdot 0.7H_2O$ in nitrogen gas (heating rate, 10°C h^{-1}; counting time for each pattern, 1000 s); *, spurious diffraction line due to the sample holder being nickel.

$Zn_3(OH)_4(NO_3)_2$, ZnO and phase X. The total amount of this latter phase is obtained at about 110°C and that of $Zn_3(OH)_4(NO_3)_2$ at 125°C. The decomposition of $Zn_3(OH)_4(NO_3)_2$ into ZnO takes place in a second stage in the temperature range 125–135°C. The third stage, slightly overlapping with the second one, concerns the decomposition of phase X into ZnO. For the reasons given above, the TG curve cannot provide valuable information. However, changes in the intensity of the line 100 of ZnO, as a function of temperature, shows that about 62%, 22% and 16% of ZnO are formed during the three successive stages. Taking into account the small overlap of the two last stages, this corresponds approximately to the formation of 3, 1 and 1 molecules of oxide, respectively. This means that, in the first stage, the precursor leads to 3 molecules of ZnO, 1/3 molecule of $Zn_3(OH)_4(NO_3)_2$ and phase X, which, in turn, gives one molecule of ZnO in the last stage. This result can be compared with that obtained for the diammine hydroxysalt.

Structural and chemical analyses of the new phase

Attempts to synthesize pure phase X were unsuccessful. Its production at the end of the first stage of the decomposition of $Zn_5(OH)_8(NO_3)_2 \cdot 2NH_3$ necessarily involves its mixture with ZnO. As a consequence, the chemical analysis of the phase X could not be performed since, moreover, gaseous

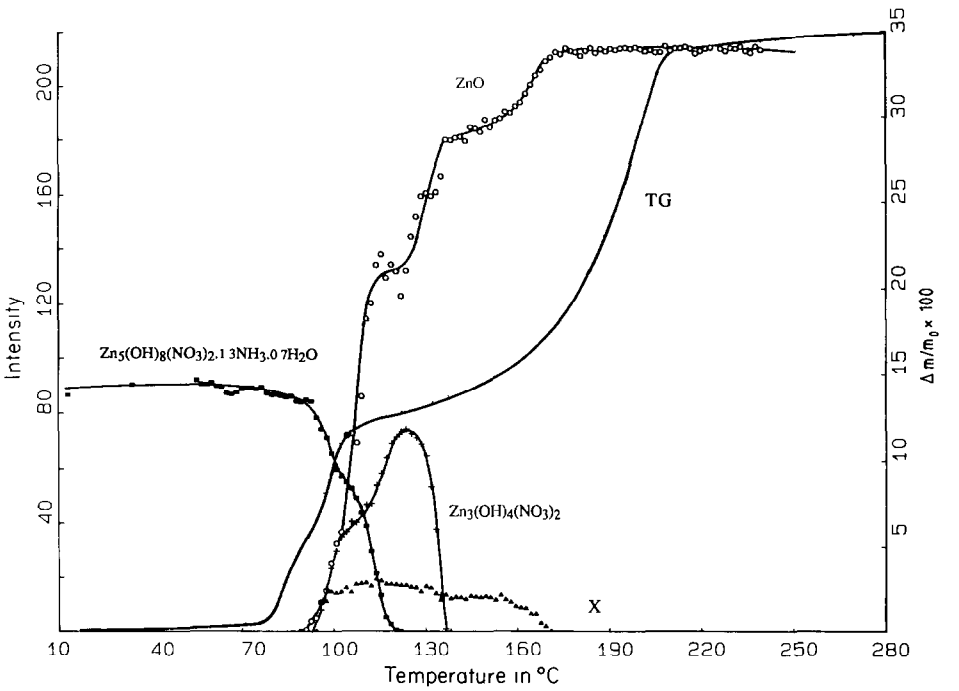

Fig. 6. Integrated intensities of selected diffraction lines vs. temperature from the thermodiffractometry of $Zn_5(OH)_8(NO_3)_2 \cdot 1.3NH_3 \cdot 0.7H_2O$ in nitrogen gas (■, 200 of $Zn_5(OH)_8(NO_3)_2 \cdot 1.3NH_3 \cdot 0.7H_2O$; +, 100 of $Zn_3(OH)_4(NO_3)_2$; ▲, 021 of ×; ○, 100 of ZnO). The full line represents the TG curve.

molecules of NO and NO_2 remain adsorbed on the finely divided ZnO and are eliminated at temperatures where X is unstable. The results of the structural and mass spectrometry studies are reported hereafter.

To prevent a transformation of the mixture phase X–ZnO, in normal atmosphere, in the course of the collection of the powder diffraction data, the sample was located in a gas-tight sample holder designed for preserving a specimen under nitrogen gas. Indexing of the powder pattern of phase X was carried out using the program DICVOL91 [11]. A unique orthorhombic solution was obtained ($M_{20} = 44$; $F_{20} = 66(0.0055; 55)$). The complete powder diffraction data were reviewed by means of the program NBS*AIDS83 [12] yielding the refined unit cell parameters $a = 10.2906(1)$ Å, $b = 11.4705(15)$ Å, $c = 5.8193(9)$ Å, $V = 686.9(1)$ Å^3, with the corresponding figures of merit $M_{20} = 67$ and $F_{30} = 74(0.0052; 78)$. X-Ray powder diffraction data of phase X are listed in Table 2. An attempt to solve the crystal structure from the powder diffraction pattern was performed. On the basis of 171 reflections available in the angular range 10–74° (2θ), a total pattern decomposition program was used to generate a list of structure factors from which a Patterson map was calculated. Its interpretation allowed us to identify a unique Zn atom in the asymmetric unit cell, according to the space groups

TABLE 2

X-ray powder diffraction data for phase X

$h\,k\,l$	$2\theta_{obs}$/deg	$2\theta_{calc}$/deg	d_{obs}/Å	I_{obs}	$h\,k\,l$	$2\theta_{obs}$/deg	$2\theta_{calc}$/deg	δ_{obs}/Å	I_{obs}
0 1 0	11.540	11.543	7.66	15	3 1 2	41.411	41.414	2.1787	4
0 2 0	15.429	15.437	5.74	27	4 2 1	41.447	41.447	2.1769	8
2 0 0	17.221	17.220	5.14	4	1 5 1	43.265	43.259	2.0895	2
1 1 1	19.130	19.138	4.64	4	0 4 2	44.308	44.315	2.0427	5
0 2 1	21.731	21.739	4.086	100	4 0 2	47.115	47.116	1.9273	12
2 2 0	23.204	23.206	3.830	15	3 3 2	47.365	47.329	1.9178	4
1 3 0	24.821	24.822	3.584	27	4 2 2	49.886	49.876	1.8266	2
3 1 0	27.117	27.112	3.286	4	4 4 1	50.107	50.108	1.8190	14
2 2 1		27.865			2 1 3		50.894		
	27.863		3.199	25		50.916		1.7920	3
0 3 1		27.898			2 6 0		50.915		
1 3 1	29.242	29.241	3.052	2	1 5 2	51.452	51.455	1.7746	4
0 0 2	30.699	30.703	2.910	15	2 2 3		52.864		
						52.867		1.7304	5
0 4 0	31.162	31.164	2.868	17	5 3 1		52.871		
3 1 1	31.232	31.232	2.862	17	6 0 0	53.371	53.376	1.7152	2
1 1 2	32.889	32.902	2.721	2	2 6 1		53.457		
						53.445		1.7130	2
0 2 2	34.548	34.538	2.594	4	4 5 0		53.470		
0 4 1	34.847	34.846	2.572	4	3 1 3		54.919		
						54.940		1.6699	7
3 3 0	35.121	35.118	2.553	4	3 6 0		54.940		
2 0 2	35.411	35.413	2.533	2	5 1 2	55.204	55.205	1.6625	<1
4 2 0	38.315	38.315	2.3473	20	5 4 1		57.284		
						57.305		1.6065	8
3 3 1	38.462	38.470	2.3387	1	0 4 3		57.296		
2 2 2		38.838			3 5 2	57.718	57.759	1.5960	3
	38.845		2.3165	3					
0 3 2		38.863			4 1 3		60.246		
						60.268		1.5344	11
2 4 1	39.125	39.121	2.3005	3	4 6 0		60.265		
1 3 2	39.875	39.875	2.2590	8	2 6 2	60.672	60.640	1.5251	<1
1 5 0	40.237	40.244	2.2395	4	4 2 3	62.014	62.016	1.4953	4

Cmcm or $Cmc2_1$. The refinement by the Rietveld method of both the structural model of ZnO and the heavy atom coordinates (0.35, 0.176, 0.75) of phase X yielded structure model indicators R_F of 2% and 19%, respectively. Unfortunately, subsequent Fourier syntheses did not allow us to establish a definitive and complete structural model for phase X, which could have been a means for determining its chemical formula. This can be attributed to the uncertainty on the intensity of Bragg reflections of phase X due to the dominant contribution of ZnO in the observed X-ray powder diffraction pattern.

Figure 7 shows the changes of the relative intensities of H_2O^+, NH_2^+, NO^+ and NO_2^+ as a function of temperature during the course of the decomposition of $Zn_5(OH)_8(NO_3)_2 \cdot 2NH_3$ in high vacuum, obtained from

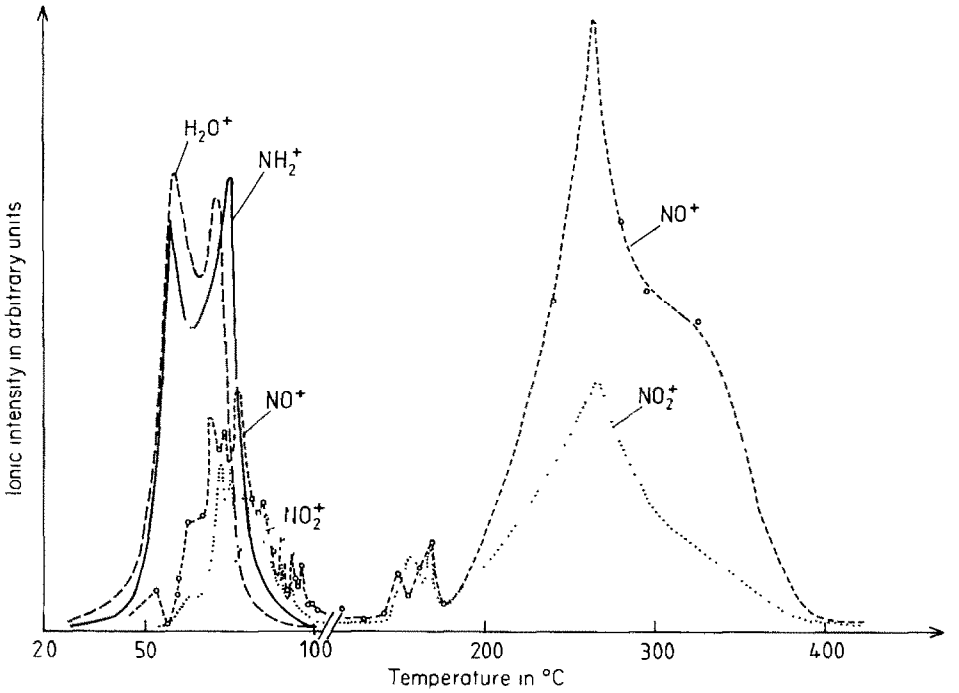

Fig. 7. Relative intensities of H_2O^+ (– – –), NH_2^+ (——), NO^+ (– – –) and NO_2^+ (·····) vs. temperature from mass spectrometry analysis during the decomposition of $Zn_5(OH)_8(NO_3)_2 \cdot 2NH_3$ (pressure, 10^{-7} mbar; heating rate, 100°C h^{-1}).

mass spectrometric analysis. The ions H_2O^+, NH_2^+, NO^+ and NO_2^+ are representative of the gases H_2O, NH_3, NO and NO_2, respectively. It is obvious that the decomposition in vacuum proceeds in two strongly superimposed stages and ends at about 100°C, as confirmed by complementary thermodiffractometry studies. The two maxima observed, at 57°C and 75°C, for NH_2^+ and H_2O^+ correspond to the first and the second stage of the decomposition. This indicates that phase X releases H_2O and NH_3 during its decomposition. By contrast, it can be noted that the two maxima for NH_2^+ have similar intensities indicating that about the same amount of NH_3 is produced in the two stages. The release of NO and NO_2 is delayed with respect to that of H_2O and NH_3, and may be due to adsorption effects on zinc oxide. Figure 7 clearly shows that the desorption of these two gases which seems to be difficult at low temperature, occurring in successive jumps, becomes important only beyond 200°C. The strong adsorption of NO and NO_2 on ZnO should be related to the microstructure of this oxide whose crystallites are of about 250 Å as deduced from an X-ray diffraction line profile analysis. Therefore, this spectrometry study demonstrates that phase X contains OH^-, NO_3^- and NH_3 groups. In conclusion, taking into account the results of the structural, mass spectrometry and thermo-

diffractometry analyses, the most simple probable chemical formula for phase X is $Zn(OH)(NO_3) \cdot NH_3$.

CONCLUSION

This study has shown that the substitution of H_2O by NH_3 molecules in the hydroxide nitrate $Zn_5(OH)_8(NO_3)_2 \cdot 2H_2O$ can be partial or complete. Although the ammines obtained are isostructural with the dihydrate, the substitution rate induces wide modifications in their thermal decomposition process. The thermal decomposition of $Zn_5(OH)_8(NO_3)_2 \cdot 2H_2O$ takes place in three well defined stages where $Zn_5(OH)_8(NO_3)_2$, the mixture $Zn_3(OH)_4(NO_3)_2$ and ZnO, and ZnO are successively formed. On the contrary, the aquo-ammine decomposes through three more complicated stages. The first stage is characterized by the simultaneous formation of ZnO, $Zn_3(OH)_4(NO_3)_2$ and a new ammine zinc hydroxide nitrate with the suggested chemical formula $Zn(OH)(NO_3) \cdot NH_3$. In the two following stages, the decompositions of $Zn_3(OH)_4(NO_3)_2$ and $Zn(OH)(NO_3) \cdot NH_3$ into ZnO slightly overlap, $Zn(OH)(NO_3) \cdot NH_3$ appearing as thermally the more stable compound. Lastly, the diammine decomposes in two stages only. In the first, ZnO and $Zn(OH)(NO_3) \cdot NH_3$ appear simultaneously, this latter leading to ZnO in the second. Finally, this study points out that the dihydrated precursor provides the anhydrous compound $Zn_5(OH)_8(NO_3)_2$ in the first stage of the decomposition and that it is necessary that the precursor be at least partially hydrated to generate $Zn_3(OH)_4(NO_3)_2$. It shows also that $Zn(OH)(NO_3) \cdot NH_3$ is an intermediate compound in the decomposition of the ammines.

This study shows that sequential diffractometry is a very useful tool for understanding complex decomposition processes of materials. It is complementary to other conventional thermal analysis methods such as thermogravimetry and mass spectrometry, especially when an adsorption phenomenon occurs during the course of the transformations.

REFERENCES

1 M. Louër, D. Louër and D. Grandjean, Acta Crystallogr., Sect. B, 29 (1973) 1969.
2 D. Louër, J.P. Auffrédic, J.I. Langford, D. Ciosmak and J.C. Niepce, J. Appl. Crystallogr., 16 (1983) 183.
3 D. Louër, R. Vargas and J.P. Auffrédic, J. Am. Ceram. Soc., 67(2) (1984) 136.
4 W. Stählin and H.R. Oswald, Acta Crystallogr., Sect. B, 26 (1970) 860.
5 W. Stählin and H.R. Oswald, J. Solid State Chem., 3 (1971) 256.
6 P. Bénard, J.P. Auffrédic and D. Louër, Powder Diffr., submitted for publication.
7 Y.M. de Haan, Nature, 200 (1963) 876.
8 J. Plévert, J.P. Auffrédic, M. Louër and D. Louër, J. Mater. Sci., 24 (1989) 1913.
9 D. Louër and J.I. Langford, J. Appl. Crystallogr., 21 (1988) 430.
10 J.P. Auffrédic and D. Louër, J. Solid State Chem., 46 (1983) 245.
11 A. Boultif and D. Louër, J. Appl. Crystallogr., 24 (1991) 987.

12 A.D. Mighell, C.R. Hubbard and J.K. Stalick, NBS*AIDS80: a FORTRAN program for crystallographic data evaluation, Natl. Bur. Stand. (U.S.), Tech. Note, 1141 (1981) (NBS*AIDS83 is an expanded version of NBS*AIDS80.)